



Mechanical fatigue of human red blood cells

Yuhao Qiang^a, Jia Liu^a, Ming Dao^{b,1}, Subra Suresh^{c,1}, and E. Du^{a,d,1}

^aDepartment of Ocean and Mechanical Engineering, Florida Atlantic University, Boca Raton, FL 33431; ^bDepartment of Materials Science and Engineering, Massachusetts Institute of Technology, Cambridge, MA 02139; ^cNanyang Technological University, Republic of Singapore 639798; and ^dDepartment of Biological Sciences, Florida Atlantic University, Boca Raton, FL 33431

Contributed by Subra Suresh, August 15, 2019 (sent for review June 17, 2019; reviewed by Guruswami Ravichandran and M. Taher A. Saif)

Fatigue arising from cyclic straining is a key factor in the degradation of properties of engineered materials and structures. Fatigue can also induce damage and fracture in natural biomaterials, such as bone, and in synthetic biomaterials used in implant devices. However, the mechanisms by which mechanical fatigue leads to deterioration of physical properties and contributes to the onset and progression of pathological states in biological cells have hitherto not been systematically explored. Here we present a general method that employs amplitude-modulated electrodeformation and microfluidics for characterizing mechanical fatigue in single biological cells. This method is capable of subjecting cells to static loads for prolonged periods of time or to large numbers of controlled mechanical fatigue cycles. We apply the method to measure the systematic changes in morphological and biomechanical characteristics of healthy human red blood cells (RBCs) and their membrane mechanical properties. Under constant amplitude cyclic tensile deformation, RBCs progressively lose their ability to stretch with increasing fatigue cycles. Our results further indicate that loss of deformability of RBCs during cyclic deformation is much faster than that under static deformation at the same maximum load over the same accumulated loading time. Such fatigue-induced deformability loss is more pronounced at higher amplitudes of cyclic deformation. These results uniquely establish the important role of mechanical fatigue in influencing physical properties of biological cells. They further provide insights into the accumulated membrane damage during blood circulation, paving the way for further investigations of the eventual failure of RBCs causing hemolysis in various hemolytic pathologies.

mechanical fatigue of biological cells | mechanical fatigue of erythrocytes | fatigue-induced damage | cyclic loading | static loading

Fluctuations and repeated cyclic variations in mechanical loads or strains lead to the onset, subcritical growth, and eventual catastrophic failure of engineered materials (1). Deterioration of physical properties, structural integrity, and functional performance arising from this mechanical fatigue effect is a major consideration in the design of materials and components used in a wide spectrum of engineering applications including buildings, roads, bridges, and other civil infrastructure, aircraft, automotive parts, marine structures, pressure vessels, pipelines, and coatings used for thermo-mechanical protection. These considerations of mechanical fatigue have given rise to stringent guideline standards for the design and routine maintenance of human life-critical and safety-critical structures and components such as commercial passenger aircraft (1, 2). Practical implications of mechanical fatigue in daily life and its technological and economic consequences for industry and society have led to considerable scientific research over many decades into the mechanisms of cyclic deformation, fatigue crack initiation, subcritical flaw propagation, and final fracture in a wide variety of materials. These studies in engineering materials have demonstrated significantly more deleterious effects of cyclic loads on the creation and propagation of damage and cracking than those seen under sustained or monotonically varying loads or strains of the same maximum intensity imposed for the same duration of time (see, e.g., a comprehensive literature review of mechanisms, mechanics, and practical implications of fatigue in ref. 1). Exacerbation of damage evolution in metal alloys under

fluctuating loads stems from to-and-fro motion of defects which typically leads to the localization of deformation around preferential crystallographic orientations, shear planes and directions, free surfaces, and sites of stress concentrators. This process is aided by continual changes in the underlying material structure and substructure to promote cycle-by-cycle accumulation of fatigue damage which advances subcritically until catastrophic fracture occurs (1).

Mechanical fatigue of engineering components used in load-bearing structures and its consequences in the presence of elevated or low temperatures, corrosive environments, irradiation, thermal fluctuations, and residual stresses have been the primary focus of scientific studies for more than a century (1). With advances in microelectronics and microelectromechanical systems, thermal fatigue and mechanical fatigue of thin films and multilayered materials have also evolved as a subject of scientific investigation for material design, reliability prediction, and analysis of the integrity of functional devices (3). More recently, numerous studies have identified the role of fatigue in influencing the structure, properties, and performance of natural and synthetic biomaterials as, for example, in the case of mineralized human tissues such as cortical bone and dentin (4), orthopedic (1) and dental implants (5), synthetic heart valves (6), and hydrogels (7) used in tissue engineering, personal care, and medicine.

Biological cells, such as human red blood cells (RBCs), undergo significant cyclic deformation through large elastic stretching and relaxation as they squeeze through and traverse microvasculature and other size-limiting pathways to perform their biological

Significance

The mechanisms underlying degradation of biological cells due to mechanical fatigue are not well understood. Specifically, detrimental effects of fatigue on properties and homeostasis of human red blood cells (RBCs), as they repeatedly deform while traversing microvasculature, have remained largely unexplored. We present a general microfluidics method that incorporates amplitude-modulated electrodeformation to induce static and cyclic mechanical deformation of RBCs. Fatigue of RBCs leads to significantly greater loss of membrane deformability, compared to static deformation under the same maximum load and maximum-load duration. These findings establish unique effects of cyclic mechanical deformation on the properties and function of biological cells. Our work provides a means to assess the mechanical integrity and fatigue damage of RBCs in blood circulation.

Author contributions: M.D., S.S., and E.D. designed research; Y.Q. and J.L. performed research; Y.Q., J.L., M.D., S.S., and E.D. analyzed data; and Y.Q., M.D., S.S., and E.D. wrote the paper.

Reviewers: G.R., California Institute of Technology; and M.T.A.S., University of Illinois at Urbana-Champaign.

The authors declare no conflict of interest.

This open access article is distributed under [Creative Commons Attribution-NonCommercial-NoDerivatives License 4.0 \(CC BY-NC-ND\)](https://creativecommons.org/licenses/by-nc-nd/4.0/).

¹To whom correspondence may be addressed. Email: mingdao@mit.edu, ssuresh@ntu.edu.sg, or edu@fau.edu.

This article contains supporting information online at www.pnas.org/lookup/suppl/doi:10.1073/pnas.1910336116/-DCSupplemental.

First published September 16, 2019.

disk-shaped RBCs at the 4 voltages, for fatigue loading cycles $N = 1, 50, 450,$ and 900 . Regions highlighted in gray show cell shapes in the fully relaxed state and those in purple show the fully deformed state. Within the initial 50 cycles, cells were able to completely recover their initial disk shape upon unloading from the peak load. Permanent deformation in cell membranes started to occur only after about 450 fatigue cycles and continued for the remainder of cyclic loading. The extent of permanent deformation was higher at the higher voltages of 1.0 V and 1.2 V, as seen in Fig. 1C. Cell morphological change is quantified by the stretch ratio S_R , which is the ratio of the major axis, a , to the minor axis, b , of the cell fitted by an ellipse. Evolution of S_R values of 4 representative RBCs deformed by 0.5, 0.8, 1.0, and 1.2 V are plotted as functions of time, respectively (SI Appendix, Fig. S2 A–D). As seen in SI Appendix, Fig. S2, the time required for cells to attain a plateau in maximum S_R and the time for full relaxation extend significantly into many cycles of fatigue loading. These findings suggest that the deleterious effects of cyclic loads on RBC membrane damage are manifested only after a critical number of cycles and that they accumulate over hundreds of fatigue cycles. Permanent damage in cell membranes is consistently observed when the voltage level is in excess of 0.5 V. The characteristic features of fatigue damage in RBC membranes include pronounced shape changes from a disk shape into elliptocyte, stomatocyte, or knizocyte-like shapes, as well as the development of single to multiple thorny projections on cell membranes (SI Appendix, Fig. S2E).

Degradation in Mechanical Properties of RBCs. We characterized the mechanical properties of RBC membranes in response to different levels of shear stresses calibrated from different voltage values. Details of shear stress calibration can be found elsewhere (23). A brief description of our constitutive models for the viscoelastic deformation characteristics of RBCs and of the cell-membrane shear stresses is presented in SI Appendix, *Constitutive Model for Viscoelastic Deformation of RBC Membranes*. The applied voltage was kept at no more than 2.0 V to prevent any possible membrane damage that may occur outside of mechanical fatigue. For this reason, the loading was kept below certain threshold levels: a threshold electrical field strength of 2.1 kV/cm (24) and mechanical stress on the membrane of 150 Pa (25). For an assumed membrane thickness of 10 nm, the corresponding values of RBC membrane shear stresses were calculated to be 1.19 ± 0.22 Pa, 1.87 ± 0.42 Pa, 2.85 ± 0.77 Pa, 4.78 ± 1.48 Pa, and 9.63 ± 3.21 Pa for the applied voltages of 0.8, 1.0, 1.2, 1.5, and 2.0 V, respectively.

The dynamic deformation of RBCs is characterized by the transient value of the principal extension/contraction ratio, $\lambda(t)$, which is calculated by dividing the initial value of the minor axis, b_0 , by its transient value, $b(t)$.* Fig. 2A shows the instantaneous value of λ as a function of number of fatigue cycles, N , for a particular

*Note that $\lambda(t)$ is defined here in terms of the instantaneous value of the contraction ratio in the transverse direction of tensile cyclic loading, $b_0/b(t)$, rather than as the axial extension ratio, $a(t)/a_0$. This is because a small part of the deformed membrane along the tensile loading axis of axial dimension a is necessarily obstructed from view by the gold electrode when imaging the cell. This partial obstruction could lead to some error in the analysis of deformation if the latter definition of $\lambda(t)$ along the axial direction had been invoked. In SI Appendix, we demonstrate that the definition and choice of the instantaneous values of extension ratio based either on the axial extension ratio, $a(t)/a_0$, or the corresponding transverse contraction ratio, $b_0/b(t)$, has absolutely no effect on the trends discovered here about the role of mechanical fatigue in influencing the behavior of RBCs. There are, however, some anticipated differences in the quantitative values of key parameters characterizing mechanical fatigue effects between the 2 related definitions of actual values of $\lambda(t)$ because of the normal variations in cell response in this mutually orthogonal directions and the experimental scatter and errors in extracting axial and transverse dimensions during deformation from optical images. Because of the relatively greater accuracy of the former definition, $\lambda(t) = b_0/b(t)$, in the experimental measurements, all subsequent results on the principal extension ratio are presented in the paper, with this choice of definition. For completeness, we present all of the corresponding results obtained using the alternative definition of axial extension ratio, $a(t)/a_0$, in SI Appendix and demonstrate that none of the trends and conclusions reported here is unaffected by the particular choice of the definition of the extension ratio.

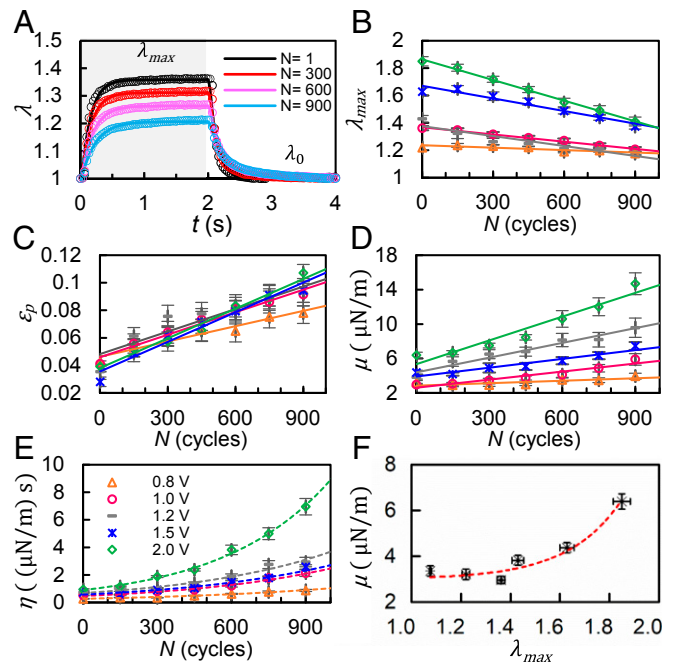


Fig. 2. Degradation of mechanical properties of RBCs under cyclic tensile loading of constant amplitude. (A) Instantaneous values of λ averaged from individually tracked cells ($n = 20$) in both stretching phase (gray region) and relaxation phase (white region) for $N = 1, 300, 600,$ and 900 fatigue cycles at 1.0 V. Open circles represent experimental measurement and the solid curves represent exponential fit to the data. (B–E) Variation of the mean value of λ_{\max} , ϵ_p , μ , and η , respectively, of RBCs with the number of fatigue loading cycles, N , for 5 different voltage levels of 0.8, 1.0, 1.2, 1.5, and 2.0 V (represented by the same set of symbols as shown in E). (F) Nonlinearity in membrane shear modulus, μ , plotted as a function of λ_{\max} at $N = 1$. The solid lines represent the best fit linear regression lines. The dashed lines represent the best fit exponential curves. Error bars indicate standard error of the mean (SEM).

voltage of 1.0 V. Values of λ during the stretching phase and the relaxation phase can be fitted well with an exponential function, $\lambda = A \times \exp(B \times t) + C$, for each cycle. We extract the maximum extension (λ_{\max}) and the minimum extension (λ_0) in the fully stretched and fully relaxed states, respectively. The initial value of λ_{\max} indicated by the vertical intercept ($\tilde{\lambda}_{\max}$) increases with the voltage level as a result of higher resulting stresses, with the best-fit linear regression, $\tilde{\lambda}_{\max} = 0.53 \times V + 0.82$, with $R^2 = 0.96$. Mean values of λ_{\max} decrease from 1.36 for $N = 1$ to 1.32, 1.27, and 1.21 for $N = 300, 600,$ and 900 , respectively.

The value of λ_{\max} strongly varies with the number of loading cycles for all stress levels. The best-fit linear regressions are $\lambda_{\max} = -8 \times 10^{-5} \times N + 1.25$ with $R^2 = 0.90$ for 0.8 V, $\lambda_{\max} = -2 \times 10^{-4} \times N + 1.37$, with $R^2 = 0.99$ for 1.0 V, $\lambda_{\max} = -2 \times 10^{-4} \times N + 1.38$, with $R^2 = 0.85$ for 1.2 V, $\lambda_{\max} = -3 \times 10^{-4} \times N + 1.67$, with $R^2 = 0.95$ for 1.5 V, and $\lambda_{\max} = -5 \times 10^{-4} \times N + 1.86$ with $R^2 = 1.0$ for 2.0 V, as shown in Fig. 2B. Additionally, the magnitude of the negative slope (m) of the lines decreases with increasing voltage, with the best-fit linear regression, $m = 3 \times 10^{-4} \times V - 2 \times 10^{-4}$, with $R^2 = 0.97$. These results indicate that the rate of mechanical damage of the cell membrane is proportional to the intensity of cyclic deformation which, in turn, depends on the magnitude of voltage.

In order to quantify and compare the extent of fatigue damage arising among the different cases, permanent deformation in RBC membrane during fatigue was evaluated by the effective plastic strain, $\epsilon_p = (S_{R_{\min}}(N) - 1/S_{R_{\min}}(N))/4$, where $S_{R_{\min}}$ denotes the minimum stretch ratio in fully relaxed state. The mean value of ϵ_p is proportional to the number of loading cycles ($R^2 > 0.9$; Fig. 2C). The slope of the linear functions increases with the voltage level,

ratio, $\lambda_{\max}^* = \lambda_{\max} / \lambda_{\max, t=0}$. This represents the ratio of the instantaneous value of the relative extension ratio, λ_{\max} , of the RBC to that of the initial value of λ_{\max} at time $t = 0$. Fig. 4 shows the changes in λ_{\max}^* as a function of accumulated time under maximum load for static loading for the imposed voltages of 1.2 and 2 V in comparison to those under cyclic loading for the 2 frequencies with a rectangular waveform. This figure establishes that cyclic loading leads to a significantly greater reduction in the deformability of the cells than static loading. At the larger load, the lower-frequency cyclic loading (longer loading time) shows a relatively smaller loss in deformability (and a trend closer to that of the static loading case). The relative loss of deformability of RBCs under cyclic loading was as much as $11.9 \pm 0.01\%$ for 1.2 V and $21.7 \pm 0.02\%$ for 2 V, compared to the static loading case. The actual variation of λ_{\max} as a function of time is shown in *SI Appendix, Fig. S5*.

Effect of Loading Waveform on Mechanical Fatigue. As strain rate is an important variable, along with strain, for the characterization of viscoelastic behavior of cell membranes (35, 36), we examined the effect of waveform (for a fixed cyclic loading frequency of 0.25 Hz). For this purpose, we compared mechanical fatigue with a rectangular waveform to that with a half-wave rectified (HWR) sinusoidal waveform. This latter waveform was achieved by modulating the amplitude of the 1.58-MHz carrier wave, $V = 1.2\sin(\pi t/2)$, with the period of 4 s, which comprised a 2-s duration of loading time (*SI Appendix, Fig. S6A* and *Movie S4*) and an equal time for unloading (with the voltage turned off) and relaxation. *SI Appendix, Fig. S6B* shows the instantaneous S_R values of RBC membranes, averaged from 22 measurements, as a function of time at fatigue loading cycles, $N = 1, 300, 450, 600,$ and 900 . We observed that cell membranes gradually deformed to a maximum S_R and then gradually relaxed to a minimum during each cycle. The 2-s relaxation interval was sufficient for deformed cell membranes to fully recover their shape before the next loading cycle.

Similar to the fatigue characteristics of cell membranes under rectangular-waveform cyclic loading, the maximum S_R values for the sinusoidal loading was found to decrease with the number of loading cycles while the minimum S_R increased along with the loading cycles (*SI Appendix, Fig. S6B*). The peaks of the S_R shifted and showed a greater hysteresis of membrane cyclic deformation with increasing fatigue cycles (marked by the dashed line in *SI*

Appendix, Fig. S6A). The lag between the peak stress and peak deformation S_R increased approximately from 0 s at $N = 1$ to 0.13 s at $N = 900$, indicating an increase in viscosity of the cell membrane. To quantify the membrane viscosity, the characteristic time t_c was determined from the relaxation process when the external force was removed, using *SI Appendix, Eq. 9* similarly to that used to obtain *SI Appendix, Fig. S3*. A significant rise in t_c was noticed, from 0.16 s to 0.43 s in ~ 900 loading cycles.

Fig. 5A shows the stress-strain (σ - ϵ) hysteresis loops of cell membranes. The maximum shear strain decreased gradually from 0.96 at $N = 1$ to 0.84, 0.74, 0.59, and 0.53 at $N = 300, 450, 600,$ and 900 , respectively. More importantly, we observed appreciable progressive change in the dissipated hysteresis energy E , determined from the enclosed area of the fatigue hysteresis loop. During the initial 300 loading cycles, the value of E remained approximately constant at 0.20 to 0.21 $\mu\text{J}/\text{m}^2$ and then gradually increased to 0.31 $\mu\text{J}/\text{m}^2$ for $N = 450$ before attaining a plateau value of $\sim 0.40 \mu\text{J}/\text{m}^2$ between $N = 600$ and $N = 900$. Correlation between the dissipated energy E and the number of loading cycles was strong with $R^2 = 0.99$, with the best-fit Boltzmann growth line given by the expression $E = 0.4 / 0.2 / (1 + \exp((N - 445)/50)) \mu\text{J}/\text{m}^2$. The total dissipated energy up to the inflection point ($N = 445$ cycles) was estimated to be 96 $\mu\text{J}/\text{m}^2$, which is on the order of the energy, 80 $\mu\text{J}/\text{m}^2$, required for dissociation between the phospholipid bilayer of the RBC membrane and its cytoskeletal comprising the spectrin network (15). The values of ϵ_p , μ , and η for the HWR sinusoidal waveform loading were compared to those for the rectangular waveform loading (Fig. 5 B-D). The membrane shear modulus is higher in the case of rectangular waveform loading than that for the sinusoidal amplitude loading. Here, the shear modulus for the former became significantly higher after 300 loading cycles ($P < 0.001$). However, η is not significantly different between the 2 different waveforms ($P > 0.05$ after 900 cycles). Furthermore, the evolution of permanent deformation, ϵ_p , in cell membranes was significantly faster for the rectangular waveform than for the sinusoidal waveform ($P < 0.05$ after 300 cycles).

Discussion and Concluding Remarks

In this work, we demonstrated a mechanical fatigue testing method for biological cells, using a microfluidics-based, amplitude-modulated, electrodeformation technique. The fatigue testing platform features multiple and unique advantages for the quantitative characterization of fatigue of single biological cells. The strengths of the method lie in its simplicity and flexibility to impose controlled mechanical loads (through positive DEP) at selected frequencies and waveforms, and its capability to probe a number of single cells over thousands of fatigue cycles. In this paper, we have presented results here that quantitatively establish the following results and mechanistic insights:

- 1) Repeated cyclic loading of healthy human RBCs under well-controlled loads, cyclic frequency, and waveform leads to an intrinsic mechanical fatigue effect in the biological cell. Our experimental method provides a unique means of quantifying cyclic deformation characteristics along and transverse to the loading direction (in *SI Appendix, Figs. S8 and S9* and here in the main text) and their implications for the properties and performance of RBCs.
- 2) Mechanical fatigue of RBCs leads to a much more pronounced effect on the physical properties such as deformability, membrane shear modulus, and membrane viscosity than static loading of the same maximum voltage or load imposed on the cell for the same accumulated loading time.
- 3) Mechanical fatigue leads to hysteresis and energy dissipation of a magnitude that could be sufficient to cause dissociation of the cell membrane from its cytoskeleton, and that permanent strains progressively accumulate with fatigue cycling. These results illustrate how continued mechanical fatigue can be detrimental to the structural integrity, and hence the biological function, of the RBC, beyond the damage induced by static loads.

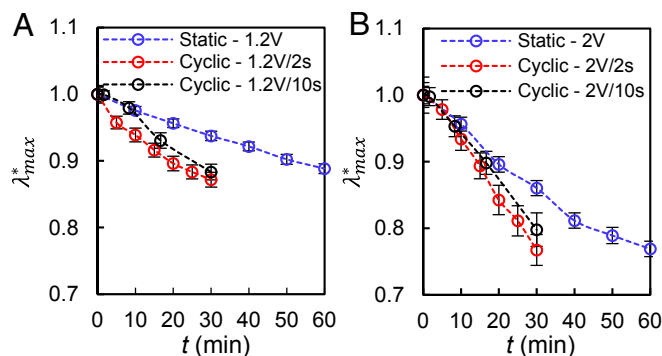


Fig. 4. Reduction of maximum relative deformation of RBCs as a function of accumulated loading time under static loading and cyclic loading with a rectangular waveform: Normalized λ_{\max}^* of healthy cells under (A) 1.2 V static loading ($n = 35$, blue circles), 1.2 V–2 s cyclic loading ($n = 58$, red circles), and 1.2 V–10 s cyclic loading ($n = 49$, black circles) and (B) 2.0 V static loading ($n = 27$, blue circles), 2.0–2 s cyclic loading ($n = 20$, red circles), and 2.0 V–10 s cyclic loading ($n = 40$, black circles). Error bars indicate SEM. Similar results comparing maximum extension ratio along the axial direction of loading between static and cyclic loading cases are given in *SI Appendix*.

Methods

Experimental Setup. The microfluidic chips for the fatigue test were made using a polydimethylsiloxane channel with 2 interdigitated electrodes coated on glass. More details are given in *SI Appendix, Experimental Setup*.

Sample Preparation. Blood samples from healthy donors were obtained with institutional review board approval from Florida Atlantic University. All blood

samples used were deidentified prior to use in the study. More details are given in *SI Appendix, Sample Preparation*.

ACKNOWLEDGMENTS. This work was supported by National Science Foundation Grants 1635312 and 1464102. M.D. acknowledges support from NIH Grant U01HL114476. S.S. acknowledges Nanyang Technological University, Singapore, for support through the Distinguished University Professorship.

1. S. Suresh, *Fatigue of Materials* (Cambridge University Press, Cambridge, UK, ed. 2, 1998).
2. International ASTM, *Fatigue Standards and Fracture Standards* (International ASTM, West Conshohocken, PA, 2018).
3. L. B. Freund, S. Suresh, *Thin Film Materials: Stress, Defect Formation and Surface Evolution* (Cambridge University Press, Cambridge, UK, 2004).
4. J. J. Kruzic, R. O. Ritchie, Fatigue of mineralized tissues: Cortical bone and dentin. *J. Mech. Behav. Biomed. Mater.* **1**, 3–17 (2008).
5. K. Shemtov-Yona, D. Rittel, Fatigue of dental implants: Facts and fallacies. *Dent J (Basel)* **4**, E16 (2016).
6. R. H. Dauskardt, R. O. Ritchie, J. K. Takemoto, A. M. Brendzel, Cyclic fatigue and fracture in pyrolytic carbon-coated graphite mechanical heart-valve prostheses: Role of small cracks in life prediction. *J. Biomed. Mater. Res.* **28**, 791–804 (1994).
7. R. Bai, J. Yang, Z. Suo, Fatigue of hydrogels. *Eur. J. Mech. A Solid.* **74**, 337–370 (2019).
8. L. Musumeci *et al.*, Prosthetic aortic valves: Challenges and solutions. *Front. Cardiovasc. Med.* **5**, 46 (2018).
9. S. Sakuma *et al.*, Red blood cell fatigue evaluation based on the close-encountering point between extensibility and recoverability. *Lab Chip* **14**, 1135–1141 (2014).
10. M. J. Simmonds, H. J. Meiselman, Prediction of the level and duration of shear stress exposure that induces subhemolytic damage to erythrocytes. *Biorheology* **53**, 237–249 (2016).
11. T. Mizuno *et al.*, Ultrastructural alterations in red blood cell membranes exposed to shear stress. *ASAIO J.* **48**, 668–670 (2002).
12. G. Bao, S. Suresh, Cell and molecular mechanics of biological materials. *Nat. Mater.* **2**, 715–725 (2003).
13. S. Suresh, Biomechanics and biophysics of cancer cells. *Acta Biomater.* **3**, 413–438 (2007).
14. J.-B. Fournier, D. Lacoste, E. Raphaël, Fluctuation spectrum of fluid membranes coupled to an elastic meshwork: Jump of the effective surface tension at the mesh size. *Phys. Rev. Lett.* **92**, 018102 (2004).
15. Z. Peng *et al.*, Lipid bilayer and cytoskeletal interactions in a red blood cell. *Proc. Natl. Acad. Sci. U.S.A.* **110**, 13356–13361 (2013).
16. I. V. Pivkin *et al.*, Biomechanics of red blood cells in human spleen and consequences for physiology and disease. *Proc. Natl. Acad. Sci. U.S.A.* **113**, 7804–7809 (2016).
17. C. E. Riva, J. E. Grunwald, S. H. Sinclair, B. L. Petrig, Blood velocity and volumetric flow rate in human retinal vessels. *Invest. Ophthalmol. Vis. Sci.* **26**, 1124–1132 (1985).
18. F. Lang, E. Lang, M. Föllner, Physiology and pathophysiology of eryptosis. *Transfus. Med. Hemother.* **39**, 308–314 (2012).
19. A. M. Dondorp, P. A. Kager, J. Vreeken, N. J. White, Abnormal blood flow and red blood cell deformability in severe malaria. *Parasitol. Today* **16**, 228–232 (2000).
20. S. Suresh *et al.*, Connections between single-cell biomechanics and human disease states: Gastrointestinal cancer and malaria. *Acta Biomater.* **1**, 15–30 (2005).
21. J. Narla, N. Mohandas, Red cell membrane disorders. *Int. J. Lab. Hematol.* **39** (suppl. 1), 47–52 (2017).
22. Y. Qiang, J. Liu, E. Du, Dynamic fatigue measurement of human erythrocytes using dielectrophoresis. *Acta Biomater.* **57**, 352–362 (2017).
23. Y. Qiang, J. Liu, F. Yang, D. Dieujuste, E. Du, Modeling erythrocyte electro-deformation in response to amplitude modulated electric waveforms. *Sci. Rep.* **8**, 10224 (2018).
24. E. H. Serspersu, K. Kinostira, T. Y. Tsong, Reversible and irreversible modification of erythrocyte membrane permeability by electric field. *Biochim. Biophys. Acta* **812**, 779–785 (1985).
25. L. B. Leverett, J. D. Hellums, C. P. Alfrey, E. C. Lynch, Red blood cell damage by shear stress. *Biophys. J.* **12**, 257–273 (1972).
26. Y. Qiang, J. Liu, E. Du, Dielectrophoresis testing of nonlinear viscoelastic behaviors of human red blood cells. *Micromachines (Basel)* **9**, 21 (2018).
27. J. P. Mills *et al.*, Effect of plasmodial RESA protein on deformability of human red blood cells harboring *Plasmodium falciparum*. *Proc. Natl. Acad. Sci. U.S.A.* **104**, 9213–9217 (2007).
28. H. Zhang, K.-K. Liu, Optical tweezers for single cells. *J. R. Soc. Interface* **5**, 671–690 (2008).
29. R. M. Hochmuth, R. E. Waugh, Erythrocyte membrane elasticity and viscosity. *Annu. Rev. Physiol.* **49**, 209–219 (1987).
30. M. M. Haque, M. G. Moisescu, S. Valkai, A. Dér, T. Savopol, Stretching of red blood cells using an electro-optics trap. *Biomed. Opt. Express* **6**, 118–123 (2014).
31. S. Chien, K. L. Sung, R. Skalak, S. Usami, A. Tözere, Theoretical and experimental studies on viscoelastic properties of erythrocyte membrane. *Biophys. J.* **24**, 463–487 (1978).
32. R. M. Hochmuth, P. R. Worthy, E. A. Evans, Red cell extensional recovery and the determination of membrane viscosity. *Biophys. J.* **26**, 101–114 (1979).
33. M. Horade, C.-H. D. Tsai, H. Ito, M. Kaneko, Red blood cell responses during a long-standing load in a microfluidic constriction. *Micromachines* **8**, 100 (2017).
34. T. M. Fischer, M. Stöhr-Lissen, H. Schmid-Schönbein, The red cell as a fluid droplet: Tank tread-like motion of the human erythrocyte membrane in shear flow. *Science* **202**, 894–896 (1978).
35. Y.-Z. Yoon, J. Kotar, G. Yoon, P. Cicuta, The nonlinear mechanical response of the red blood cell. *Phys. Biol.* **5**, 036007 (2008).
36. J. Mancuso, W. Ristenpart, Stretching of red blood cells at high strain rates. *Phys. Rev. Fluids* **2**, 101101 (2017).
37. D. J. Quinn *et al.*, Combined simulation and experimental study of large deformation of red blood cells in microfluidic systems. *Ann. Biomed. Eng.* **39**, 1041–1050 (2011).
38. M. Dao, C. T. Lim, S. Suresh, Mechanics of the human red blood cell deformed by optical tweezers. *J. Mech. Phys. Solids* **51**, 2259–2280 (2003).
39. J. P. Mills, L. Qie, M. Dao, C. T. Lim, S. Suresh, Nonlinear elastic and viscoelastic deformation of the human red blood cell with optical tweezers. *Mech. Chem. Biosyst.* **1**, 169–180 (2004).
40. E. Du, M. Dao, S. Suresh, Quantitative biomechanics of healthy and diseased human red blood cells using dielectrophoresis in a microfluidic system. *Extreme Mech. Lett.* **1**, 35–41 (2014).
41. Y. C. Fung, P. Tong, Theory of the spherizing of red blood cells. *Biophys. J.* **8**, 175–198 (1968).
42. R. Skalak, A. Tozeren, R. P. Zarda, S. Chien, Strain energy function of red blood cell membranes. *Biophys. J.* **13**, 245–264 (1973).
43. N. R. Morris, E. M. Snyder, K. C. Beck, B. D. Johnson, Lung-to-lung circulation times during exercise in heart failure. *Eur. J. Appl. Physiol.* **106**, 621–627 (2009).
44. F. Padilla, P. A. Bromberg, W. N. Jensen, The sickle-unsickle cycle: A cause of cell fragmentation leading to permanently deformed cells. *Blood* **41**, 653–660 (1973).
45. E. Du, M. Diez-Silva, G. J. Kato, M. Dao, S. Suresh, Kinetics of sickle cell bio rheology and implications for painful vasoocclusive crisis. *Proc. Natl. Acad. Sci. U.S.A.* **112**, 1422–1427 (2015).
46. E. Du, M. Dao, Faster sickling kinetics and sickle cell shape evolution during repeated deoxygenation and oxygenation cycles. *Exp. Mech.* **59**, 319–325 (2019).